Theoretical Models for the Oxygen Radical Mechanism of Water Oxidation and of the Water Oxidizing Complex of Photosystem II

Per E. M. Siegbahn

Department of Physics, Stockholm University, Box 6730, S-113 85 Stockholm, Sweden

Received October 8, 1999

Hybrid density functional theory is used to study reasonably realistic models of the oxygen-evolving manganese complex in photosystem II. Since there is not yet any X-ray structure of the complex, other types of experimental and theoretical information are used to construct the model complexes. In these complexes, three manganese centers are predicted to be closely coupled by μ-oxo bonds in a triangular orientation. Using these models, the previously suggested oxygen radical mechanism for O_2 formation is reinvestigated. It is found that the oxygen radical in the S_3 state now appears in a bridging position between two manganese atoms. It is still suggested that only one manganese atom is redox-active. Instead, a number of surprisingly large trans-effects are found, which motivate the existence and define the function of the other manganese atoms in the Mn_4 cluster. Calcium has a strong chelating effect which helps in the creation of the necessary oxygen radical. In the present model the chemistry preceding the actual O−O bond formation occurs in an incomplete cube with a missing corner and with two manganese and one calcium in three of the corners. The external water providing the second oxygen of O_2 enters in the missing corner of the cube. The present findings are in most cases in good agreement with experimental results as given in particular by EXAFS.

I. Introduction

To obtain the mechanism for the formation of an oxygen molecule from water by the oxygen-evolving center of photosystem II in green plants is one of the most challenging problems in chemistry today. Despite decades of experimental studies, there are still large uncertainties concerning the detailed chemical steps of the water-oxidizing reactions. A major problem in this context is that the X-ray structure of the enzyme has not yet been obtained. Another problem is that the chemistry of these steps is so unique that it is very hard to find laboratory model reactions with any high degree of similarity to water oxidation. With this background, theory could be helpful and perhaps provide pieces of information which cannot at present be obtained from experiments. Although the structure of the water-oxidizing complex is not known, sufficient information from EXAFS is available to start model calculations. However, due to the complexity of the systems this is still an area which until recently has been considered too difficult for theoretical approaches. The development of density functional theory (DFT) has partly changed this situation, and an accurate treatment of systems of the necessary complexity is today at least possible. A first step in this direction was taken when a mechanism for water oxidation including all the relevant steps based on DFT model calculations was recently suggested.[1] In this mechanism, the formation of an oxygen radical is of fundamental importance, and it is therefore termed the oxygen radical mechanism. In the present paper the oxygen radical mechanism is elaborated further including larger and more realistic models of the Mn_4Ca water-oxidizing complex. This study shows that most parts of the previously suggested mechanism remain the same but some steps are modified. Some of the most important experimental findings are well reproduced by the present model.

From saturating flash experiments, water oxidation is known to occur in four steps.[2] The intermediates of these steps are denoted S_0−S_4, and O_2 formation occurs at S_4. The even S states of the water-oxidizing cluster are EPR visible while both S_1 and S_3* have been detected by parallel mode EPR.[3−5] In each step a photon is absorbed by the antenna pigments of the light-harvesting proteins and the energy is transferred to the photosynthetic reaction centers of photosystems I and II. At the reaction center of photosystem II a charge separation takes place, in which the chlorophyll P680 is ionized and the electron is transferred to the quinone Q_A. At this stage, $P680^+$ is rereduced by an electron coming from a tyrosine, Tyr_Z, located in the proximity of the water-oxidizing complex.[6] In this process, Tyr_Z loses a proton to become a neutral tyrosyl radical. In some way Tyr_Z is recreated by obtaining an electron and a proton in each step of water oxidation. Even though the details of this process are still under debate, this is one of the most important experimental findings on which the present model is built. Independently of the mechanism of this process, it means that the energy available to the water-oxidizing complex in each step is approximately equal to the bond strength of the Tyr_Z

(1) Siegbahn, P. E. M.; Crabtree, R. H. *J. Am. Chem. Soc.* **1999**, *121*, 117−127.

(2) Kok, B.; Forbush, B.; McGloin, M. *Photochem. Photobiol.* **1970**, *11*, 457.

(3) Dexheimer, S. L.; Klein, M. P. *J. Am. Chem. Soc.* **1992**, *114*, 2821−2826.

(4) Campbell, K. A.; Peloquin, J. M.; Pham, D. P.; Debus, R. J.; Britt, R. D. *J. Am. Chem. Soc.* **1998**, *120*, 447−448.

(5) Matsukawa, T.; Mino, H.; Yoneda, D.; Kawamori, A. *Biochemistry* **1999**, *38*, 4072−4077.

(6) Barry, B. A.; Babcock, G. T. *Proc. Natl. Acad. Sci. U.S.A.* **1987**, *84*, 7099−7103.

10.1021/ic9911872 CCC: $19.00
Published on Web 06/09/2000

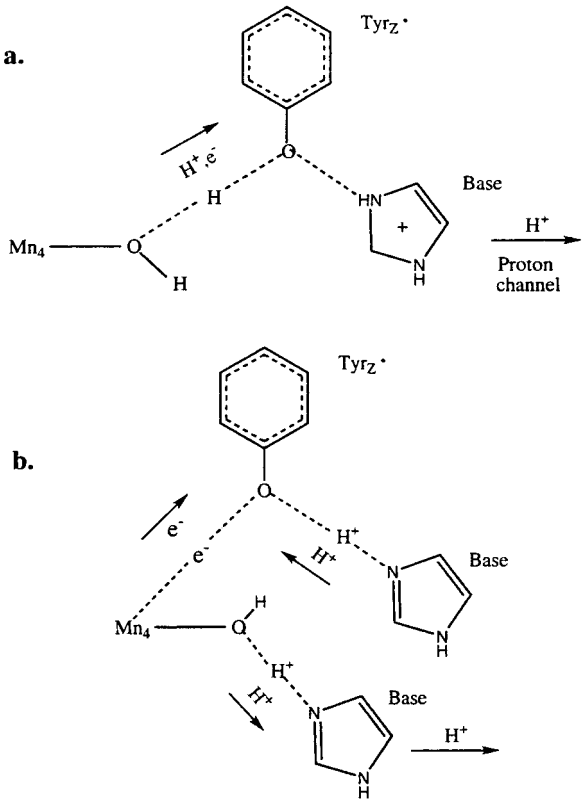

Figure 1. Schematic picture of the hydrogen abstraction scheme (a) and the electron transfer scheme (b).

O−H bond, which is equal to 86.5 kcal/mol. This energy amount can be modified, but only slightly, by changes of the charge of the cluster and changes in hydrogen bonding occurring during the S-state transitions, as discussed below. Two leading models for recreation of Tyr_Z exist. In the first model termed the hydrogen abstraction mechanism,[7] see Figure 1a, the tyrosyl radical obtains both the proton and the electron from the manganese complex in a concerted hydrogen atom transfer step. In the second model termed the electron transfer model, see Figure 1b, the tyrosyl radical obtains the electron from the manganese complex and the proton from a nearby base. In that model, the water molecules, which will eventually form O_2, will lose their protons to a different base. This model has been recently elaborated further, and some new aspects and modifications of the proton translocation mechanism have been introduced.[8] The present model for water oxidation, discussed below, is independent of which of these schemes is the correct one. Apart from the presence of the Tyr_Z radical, there are a few standard pieces of experimental information that need to be considered for any model of water oxidation. First, the water-oxidizing complex contains four manganese atoms. Second, one calcium is essential for O_2 evolution. Third, one chloride cofactor is also present but its removal does not completely inhibit O_2 evolution.

A large number of suggestions have been made over the years for the mechanism of O_2 formation, and a few of these will be mentioned here. In one mechanism the S_3 and S_4 structures were proposed to be adamantane-like Mn_4O_6 clusters. The S_4 structure was proposed to release oxygen as it rearranges to an Mn_4O_4 cluster.[9,10] On the basis of EXAFS, XANES, and EPR data, another mechanism was suggested in which only one of two manganese bis(μ-oxo) dimers in a C-shaped cluster is redox-active. In S_3 a bridging μ-oxyl radical is formed which combines with the other μ-oxo oxygen to form O_2.[9] In the hydrogen abstraction mechanism oxygen is formed from water bound to manganese as terminal rather than bridging ligands.[7] In this mechanism $Y_Z^{\bullet}$ functions as a hydrogen atom abstractor. Another characteristic feature of this model is that chloride migrates in the S_1 to S_2 and S_2 to S_3 transitions and that the function of calcium is to bind the chloride in the lower S states. In another mechanism two manganese dimers function independently, one to oxidize water to peroxide and the other to oxidize peroxide to O_2.[11] The oxidations result in the formation of a $Mn^V{=}O$ species in S_4, which is supposed to be strongly electrophilic rendering it susceptible to nucleophilic attack by a hydroxo ligand of calcium. A similar mechanism for O_2 formation is suggested in another mechanism where a chloride bridging calcium and manganese controls the nucleophilicity of the hydroxide.[12]

Although the structure of the enzyme and the detailed chemistry of the different steps are not known from experiments, a large amount of very important information of direct concern for the present study is available. Part of this information is listed here in approximate order of its impact on the present model. It should be noted that this information is obtained as sometimes debatable interpretations of experiments, and all of this information is therefore not necessarily assumed to be correct facts. The following points will be discussed and used in the modeling below:

(1) As already mentioned, in each S state the Tyr_Z radical obtains a proton and an electron, which means that the energy available for the water-oxidizing chemistry should be about 86.5 kcal/mol.[7]

(2) EXAFS experiments have been interpreted to show three Mn−Mn distances, two of them of 2.7 Å and one of 3.3 Å in the S_1 state.[9] A structure consisting of two μ-oxo-bridged Mn dimers linked in some way appears likely.

(3) Still from the EXAFS experiments, the two short Mn−Mn distances remain the same in the S_1 to S_2 transition.[9] However, in the S_2 to S_3 transition both these distances increase. This is a quite surprising result, since the cluster is oxidized, and it is a piece of information which is of critical importance for the water oxidation mechanism, as will be discussed in detail below.

(4) In the S_0 to S_1 transition,[9] one of the short Mn−Mn distances remain the same but the other one decreases from a rather long to its short distance in S_1. The matching of this fact, together with the fact mentioned under point 3, puts very high demands on a model for the water oxidation.

(7) (a) Hoganson, C. W.; Lydakis-Simantiris, N.; Tang, X.-S.; Tommos, C.; Warncke, K.; Babcock, G. T.; Diner, B. A.; McCracken, J.; Styring, S. *Photosynth. Res.* **1995**, *46*, 177. (b) Babcock, G. T. in *Photosynthesis from Light to Biosphere*; Mathis, P., Ed.; Kluwer: Dordrecht, The Netherlands, 1995; Vol. 2, p 209. (c) Tommos, C.; Tang, X.-S.; Warncke, K.; Hoganson, C. W.; Styring, S.; McCracken, J.; Diner, B. A.; Babcock, G. T. *J. Am. Chem. Soc.* **1995**, *117*, 10325.

(8) (a) Haumann, M.; Bögershausen, O.; Cherepanov, D.; Ahlbrink, R.; Junge, W. *Photosynth. Res.* **1997**, *51*, 193−208. (b) Ahlbrink, R.; Haumann, M.; Cherepanov, D.; Bögershausen, O.; Mulkidjanian, A.; Junge, W. *Biochemistry* **1998**, *37*, 1131−1142. (c) Haumann, M.; Junge, W. *Biochim. Biophys. Acta* **1999**, *1411*, 86−91.

(9) Yachandra, V. K.; Sauer, K.; Klein, M. P. *Chem. Rev.* **1996**, *96*, 2927−2950.

(10) Brudvig, G. W.; Crabtree, R. H. *Proc. Natl. Acad. Sci. U.S.A.* **1985**, *83*, 4586−4588.

(11) (a) Pecoraro, V. L. In *Manganese Redox Enzymes*; Pecoraro, V. L., Ed.; VCH: New York, 1992; pp 197−232. (b) Pecoraro, V. L.; Baldwin, M. J.; Gelasco, A. *Chem. Rev.* **1994**, *94*, 807−826. (c) Baldwin, M. J.; Gelasco, A.; Pecoraro, V. L. *Photosynth. Res.* **1993**, *38*, 303−330.

(12) Limburg, J.; Szalai, V. A.; Brudvig, G. W. *J. Chem. Soc., Dalton Trans.* **1999**, *9*, 1353−1361.

(5) Strontium EXAFS experiments have shown two Mn−Sr distances of 3.5 Å.[13] Supposedly, strontium has taken the position normally occupied by calcium. Other groups have reached different conclusions in earlier EXAFS studies.[14]

(6) So far, it has only been possible to replace the calcium cofactor by strontium and still retain activity.[15] Without calcium the normal $g = 2$ EPR multiline S_2 state is not obtained and the S_3 state cannot be reached.

(7)The chloride cofactor can be replaced by many ions and can in fact even be removed,[16] and the enzyme is still active. However, replacing chloride by fluoride stops activity. Other opinions exist about how essential chloride is for the activity.[17]

(8) Both oxygens forming O_2 are exchanging with solvent water in S_2 and S_3. One is rapidly exchanging and one is slowly exchanging,[18] indicating that the oxygens do not occupy identical chemical positions in any of these states.

(9) The active S_2 state is characterized by a $g = 2$ EPR multiline spectrum.[19] A $g = 4.1$ signal can also be obtained for an S_2 state.[20,21] In particular the $g = 4.1$ spectrum has been interpreted as showing strong interactions between more than two manganese centers.[19,22] Other interpretations exist.[23]

(10) NMR proton relaxation enhancement,[24] EPR relaxation,[25] and XANES[9,26] studies have indicated that manganese is not oxidized in the S_2 to S_3 transition. Other interpretations exist.[27,28]

(11) Experiments on the S_0 state have been interpreted to show the presence of one Mn(II) center.[29−31]

(12) The above-mentioned NMR, EPR, and XANES experiments, as well as experiments using reductants,[32,33] have been interpreted to show that the oxidation states in S_2 are $Mn^{III}Mn^{IV}{}_3$.[9] Alternative assignments, such as $Mn^{IV}Mn^{III}{}_3$, exist.[34]

(13) It has been shown that the endogenous reductant Y_D reduces the S_2 and the S_3 state with about the same rate.[35,36] In contrast, experiments using the exogenous reductant hydrazine[35] have shown that the rate of reduction is higher for the S_2 state than for the S_3 state of the cluster. This was interpreted to show that the S_3 state is very well protected against undesired reactions, presumably because it is extremely reactive at this stage.

II. Computational Details

The calculations were performed in two steps. First, an optimization of the geometry was performed using the B3LYP method.[37,38] Double-ζ basis sets were used in this step. In the second step the energy was evaluated for the optimized geometry using large basis sets including diffuse functions and with a single set of polarization functions on each atom. The final energy evaluation was also performed at the B3LYP level. All the calculations were carried out using the GAUSSIAN-94 program.[39] In the previous study,[1] polarization effects from the surrounding protein were also evaluated using a dielectric cavity model. In that study, as well as in some cases of the present study, these effects were found to be very small and were therefore not computed and are not included in the results presented below.

In the B3LYP geometry optimizations, the LANL2DZ set of the GAUSSIAN program was used. For manganese this means that a nonrelativistic ECP[40] was used. The valence basis set used for manganese in connection with this ECP is essentially of double-ζ quality. The rest of the atoms are described by standard double-ζ basis sets. In the B3LYP energy calculations the diffuse and polarization functions from the 6-311+G(1d,1p) basis sets in the GAUSSIAN program were added to the LANL2DZ basis sets. This basis set has a single set of polarization functions on all atoms, including an f-set on iron, and also diffuse functions.

When a hydrogen atom (proton and electron) is removed from a water or hydroxyl ligand of the manganese cluster, the inclusion of zero-point vibrational effects is quite important. However, for the present large molecular systems they are in practice too expensive to be directly evaluated. On the basis of previous experience, they are also quite constant from system to system. These effects were therefore taken from a smaller model used in a previous study[41] where they were found to decrease the O−H bond strength by 6.2 kcal/mol for a water ligand coordinated to a mononuclear Mn(IV) complex.

The accuracy of different DFT methods has been tested on the standard G2 benchmark test[42] consisting of 55 small first- and second-

(13) Cinco, R. M.; Robblee, J. H.; Rompel, A.; Fernandez, C.; Yachandra, V. K.; Sauer, K.; Klein, M. P. *J. Phys. Chem.* **1998**, *B102*, 8248−8256.
(14) Riggs-Gelasco, P. J.; Mei, R.; Ghanotakis, D. F.; Yocum, C. F.; Penner-Hahn, J. E. **1996**, *118*, 2400−2410.
(15) Ghanotakis, D. F.; Babcock, G. T.; Yocum, C. F. *FEBS Lett.* **1984**, *167*, 127−130.
(16) Lindberg, K.; Andreasson, L. *Biochemistry* **1996**, *35*, 14259.
(17) Wincencjusz, H.; Yocum, C. F.; van Gorkum, H. J. *Biochemistry* **1998**, *37*, 8595−8604; *Biochemistry* **1999**, *38*, 3719−3725.
(18) Messinger, J.; Badger, M.; Wydrzinski, T. *Proc. Natl. Acad. Sci. U.S.A.* **1995**, *92*, 3209−3213.
(19) Dismukes, G. C.; Siderer, Y. *Proc. Natl. Acad. Sci. U.S.A.* **1981**, *78*, 274−278.
(20) Casey, J. L.; Sauer, K. *Biochim. Biophys. Acta* **1984**, *767*, 21−28.
(21) Zimmermann, J.-L.; Rutherford, A. W. *Biochim. Biophys. Acta* **1984**, *767*, 160−167.
(22) Dubé, C. E.; Sessoli, R.; Hendrich, M. P.; Gatteschi, D.; Armstrong, W. H. *J. Am. Chem. Soc.* **1999**, *121*, 3537−3538.
(23) Åhrling, K. A.; Smith, P. J.; Pace, R. J. *J. Am. Chem. Soc.* **1998**, *120*, 13202−13214.
(24) Sharp, R. R. In *Manganese Redox Enzymes*; Pecoraro, V. L., Ed.; VCH: New York, **1992**; pp 177−196.
(25) (a) Styring, S. A.; Rutherford, A. W. *Biochemistry* **1988**, *27*, 4915−4923. (b) Evelo, R. G.; Styring, S. A.; Rutherford, A. W.; Hoff, A. J. *Biochim. Biophys. Acta* **1989**, *973*, 428−442.
(26) Roelofs, T. A.; Liang, W.; Latimer, M. J.; Cinco, R. M.; Rompel, A.; Andrews, J. C.; Sauer, K.; Yachandra, V. K.; Klein, M. P. *Proc. Natl. Acad. Sci. U.S.A.* **1996**, *93*, 3335−3340.
(27) Iuzzolini, L.; Dittmer, J.; Dörner, W.; Meyer-Klaucke, W.; Dau, H. *Biochemistry* **1998**, *37*, 17112−17119.
(28) Ono, T.; Noguchi, T.; Inoue, Y.; Kosunoki, M.; Matsushita, T.; Oyanagi, H. *Science* **1992**, *258*, 1335−1337.
(29) Guiles, R. D.; Yachandra, V. K.; McDermott, A. E.; Cole, J. L.; Dexheimer, S. L.; Britt, R. D.; Sauer, K.; Klein, M. P. *Biochemistry* **1990**, *29*, 486-496.
(30) Åhrling, K. A.; Peterson, S.; Styring, S. *Biochemistry* **1997**, *36*, 13148−13152.
(31) Messinger, J.; Robblee, J. H.; Yu, W. O.; Sauer, K.; Yachandra, V. K.; Klein, M. P. *J. Am. Chem. Soc.* **1997**, *119*, 11349−11350.
(32) (a) Renger, G. *Photosynthetica* **1987**, *21*, 203−224. (b) Renger, G. *Physiol. Plant.* **1997**, *100*, 828−841.
(33) Messinger, J.; Seaton, G. R.; Wydrzinski, T.; Wacker, U.; Renger, G. *Biochemistry* **1997**, *36*, 6862−6873.
(34) Dismukes, G. C.; Ferris, K.; Watnick, P. *Photobiochem. Photobiophys.* **1982**, *3*, 243−256.
(35) Messinger, J.; Renger, G. *FEBS Lett.* **1990**, *277*, 141−146. Messinger, J.; Wacker, U.; Renger, G. *Biochemistry* **1991**, *30*, 7852−7862.
(36) Deak, Z.; Vass, I.; Styring, S. *Biochim. Biophys. Acta* **1994**, *1185*, 65−74.
(37) Becke, A. D. *Phys. Rev.* **1988**, *A38*, 3098. Becke, A. D. *J. Chem. Phys.* **1993**, *98*, 1372. Becke, A. D. *J. Chem. Phys.* **1993**, *98*, 5648.
(38) Stevens, P. J.; Devlin, F. J.; Chablowski, C. F.; Frisch, M. J. *J. Phys. Chem.* **1994**, *98*, 11623.
(39) Frisch, M. J.; Trucks, G. W.; Schlegel, H. B.; Gill, P. M. W.; Johnson, B. G.; Robb, M. A.; Cheeseman, J. R.; Keith, T.; Petersson, G. A.; Montgomery, J. A.; Raghavachari, K.; Al-Laham, M. A.; Zakrzewski, V. G.; Ortiz, J. V.; Foresman, J. B.; Cioslowski, J.; Stefanov, B. B.; Nanayakkara, A.; Challacombe, M.; Peng, C. Y.; Ayala, P. Y.; Chen, W.; Wong, M. W.; Andres, J. L.; Replogle, E. S.; Gomperts, R.; Martin, R. L.; Fox, D. J.; Binkley, J. S.; Defrees, D. J.; Baker, J.; Stewart, J. P.; Head-Gordon, M.; Gonzalez, C.; Pople, J. A. *Gaussian 94 Revision B.2*; Gaussian Inc.: Pittsburgh, PA, 1995.
(40) Hay, P. J.; Wadt, W. R. *J. Chem. Phys.* **1985**, *82*, 299.
(41) Blomberg, M. R. A.; Siegbahn, P. E. M.; Styring, S.; Babcock, G. T.; Åkermark, B.; Korall, P. *J. Am. Chem. Soc.* **1997**, *119*, 8285−8292.
(42) Curtiss, L. A.; Raghavachari, K.; Trucks, G. W.; Pople, J. A. *J. Chem. Phys.* **1991**, *94*, 7221−7230.

row molecules.[43] A few general conclusions can be drawn from these comparisons. For the atomization energies, the B3LYP method is clearly superior to the other DFT methods with an average deviation to experiments of only 2.20 kcal/mol and a maximum error of 8.4 kcal/mol. This can be compared to the corresponding results of 1.16 and 5.1 kcal/mol, respectively, for the G2 method,[42] which is one of the most accurate ab initio methods available. Due to the lack of accurate experimental values, much less is known about the accuracy of DFT methods for transition metal complexes. However, several systematic theoretical studies have been performed on small MR^+ systems, where M is a first-row transition metal and R is H, CH_3, CH_2, or OH, with average absolute errors in calculated M−R bond energies of 3.6−5.5 kcal/mol using B3LYP.[44−46] It should be pointed out that these systems are some of the most difficult ones to treat since the atomic splittings enter directly into the bond dissociation energies in many cases. For the successive M−CO bond energies in $Fe(CO)_5^+$ and $Ni(CO)_4$, and the first M−CO bond energy in the Cr, Mo, W triad of $M(CO)_6$, B3LYP gives very good agreement with experiment, with an average error of only 2.6 kcal/mol, and the results are in most cases within the experimental error bars.[47,48] For $MnO_3(O-H)^-$, which is the only system closely related to the complexes studied in the present paper where an accurate value of an O−H bond strength is available experimentally,[49] the B3LYP result was found to be in good agreement with experiment, with values of 76.0 and 79.2 kcal/mol, respectively.[50,51,52] It can furthermore be pointed out that nonhybrid DFT methods, which do not include Hartree−Fock exchange, are not yet of sufficient accuracy to study the type of problems studied here since they give errors in computed MnO−H bond strengths of about 20 kcal/mol.[52,53]

All of the present manganese complexes have been studied using ferromagnetic coupling between the manganese centers even though they are known to be antiferromagnetically coupled. The reason is simply that convergence was never achieved for the low-spin coupling case for these systems. However, in a previous study the two coupling cases (high-spin and low-spin) were both converged for an $Mn^{IV}{}_2$−OH dimer and for an $Mn^{IV}Mn^{V}$=O dimer.[41] The results gave a lower energy for a low-spin coupling of the two Mn centers by 2.2 kcal/mol for the $Mn^{IV}{}_2$−OH dimer and by 1.8 kcal/mol for the $Mn^{IV}Mn^{V}$=O dimer. These values correspond to *J* values of 0.5 and 0.6 kcal/mol, respectively.[54] From these *J* values the correctly antiferromagnetically coupled ground states are predicted to lie 2.9 and 2.4 kcal/mol, respectively, lower than the computed ferromagnetically coupled states. From these results the O−H bond strength of the hydroxyl ligand in the $Mn^{IV}{}_2$−OH dimer can also be computed, and it is found that this bond strength is 0.5 kcal/mol stronger for the antiferromagnetic than for the ferromagnetic coupling case. This effect is well within the present error bars, which should be at least a few kcal/mol using the B3LYP method, and the neglect of antiferromagnetic coupling should therefore not affect the present conclusions. Since the total energetic effects of antiferromagnetic coupling are so small, the effects on the geometry were also found to be truly negligible, almost within the convergence thresholds used.[41]

III. Results and Discussion

The goal of the present study is to put the oxygen radical mechanism into a framework of more realistic models for the manganese cluster. Using these more realistic models, effects and requirements are studied that may be of importance for the actual cluster in the oxidation of water to O_2. To properly describe the effects found, it is necessary to give a comprehensive summary of previous findings including the oxygen radical mechanism itself. In the first subsection, the results concerning O−H bond strengths of different manganese model complexes are therefore summarized. In the second subsection, the main components and ideas of the oxygen radical mechanism are described including possible problems with this mechanism. In the subsequent subsections, the present new model complexes are discussed including the main trans-effects found. Finally, the detailed S-state transitions are described and comparisons are made between different models.

a. O−H Bond Strengths for Different Model Complexes. The most critical part in the search for a possible water oxidation mechanism is to find O−H bond strengths close to the one of 86.5 kcal/mol in tyrosine, so that a proton and an electron can be released according to one of the schemes in Figure 1. It has been shown previously[41,55] that the coordination of water and hydroxyl ligands to the manganese cluster significantly affects the O−H bond strength and can reduce it to be of suitable strength. This is clearly one of the main functions of manganese in the water oxidation process. In several previous studies the O−H bond strengths of hydroxyl and water coordinated to manganese monomer and dimer complexes have been studied in detail.[41,50,51] Since this issue is central for the water oxidation chemistry, some of the more general and also some specific results are repeated here.

In the first theoretical study of these O−H bond strengths,[41] 5-coordinated manganese monomer and dimer model complexes with hydroxyl and water ligands were used. The first O−H bond strength of an $Mn^{III}-H_2O$ monomer, leading from a water to a hydroxyl ligand, was calculated to be 83.3 kcal/mol. The second one, leading further to an Mn^{V}=O complex, was found to be 83.5 kcal/mol. These values changed only marginally when the dimer model was used, giving values of 84.3 and 85.0 kcal/mol, respectively. It may thus appear that the main part of the water oxidation mechanism, the one where the protons are removed from water, should be essentially solved. All that is required for making two Mn=O ligands is to have two 5-coordinated manganese centers. The oxo ligands should then be possible to form in the first four steps. In the final step these two Mn=O oxo ligands could combine to form O_2. Two facts complicate this simple scheme considerably. First, it turns out that formation of O_2 from two stable Mn=O oxo complexes leads to much too high barriers.[56] Second, for more realistic complexes than the simple 5-coordinated ones used previously, the second O−H bond strength leading to formation of the terminal oxo bond tends to be significantly larger than the required value of 86.5 kcal/mol. For example, it was noted already in the first study that the second O−H bond strength

(43) Bauschlicher, C. W., Jr.; Ricca, A.; Partridge, H.; Langhoff, S. R. In *Recent Advances in Density Functional Methods, Part II*; Chong, D. P., Ed.; World Scientific Publishing Co.: Singapore, **1997**, p 165.
(44) Blomberg, M. R. A.; Siegbahn, P. E. M.; Svensson, M. *J. Chem. Phys.* **1996**, *104*, 9546−9554.
(45) Ricca, A.; Bauschlicher, C. W., Jr. *J. Phys. Chem. A* **1997**, *101*, 8949−8955.
(46) Blomberg, M. R. A.; Siegbahn, P. E. M. Unpublished results.
(47) Ricca, A.; Bauschlicher, C. W., Jr. *J. Phys. Chem.* **1994**, *98*, 12899−12903.
(48) Koch, W.; Hertwig, R. H. *Encyclopedia of Computational Chemistry*; Schleyer, P. v. R., Allinger, N. L., Clark, T., Gasteiger, J., Kollman, P. A., Schaefer, H. F. III, Schreiner, P. R., Eds.; John Wiley & Sons: Chichester, U.K., 1998.
(49) Gardner, K. A.; Mayer, J. M. *Science* **1995** *269*, 1849 and private communication.
(50) Blomberg, M. R. A.; Siegbahn, P. E. M. *Theor. Chem. Acc.* **1997**, *97*, 72−80.
(51) Blomberg, M. R. A.; Siegbahn, P. E. M. *Mol. Phys.* **1999**, *96*, 571−581.
(52) Siegbahn, P. E. M.; Blomberg, M. R. A. *Annu. Rev. Phys. Chem.* **1999**, *50*, 221−249.
(53) Siegbahn, P. E. M.; Blomberg, M. R. A. *Chem. Rev.* **2000**, *100*, 421−437.
(54) Noodleman, L.; Li, J.; Zhao, X.-G.; Richardson, W. H. In *Methods in Chemistry and Materials Science*; Springborg, M., Ed.; John Wiley and Sons: New York, 1997.
(55) (a) Baldwin, M. J.; Pecoraro, V. L. *J. Am. Chem. Soc.* **1996**, *118*, 11325−11326. (b) Caudle, M. T.; Pecoraro, V. L. *J. Am. Chem. Soc.* **1997**, *119*, 3415−3416.
(56) Siegbahn, P. E. M. In *Molecular Modeling and Dynamics of Bioinorganic Systems*; Comba, P., Banci, L., Ed.; Kluwer Academic Publishers: Dordrecht, The Netherlands, 1997; pp 233−253.

increased by as much as 11.6 kcal/mol when one hydroxyl ligand was replaced by a bidentate carboxylate ligand. In general, going to a 6-coordinated $Mn^{IV}-OH$ complex, which is the preferred coordination for this oxidation state, leads to an increase of the second O−H bond strength by about 10 kcal/mol even if the product $Mn^{V}=O$ oxo complex is kept 5-coordinated (with one ligand in the second shell). If the oxo complex would have been 6-coordinated, the energetic effect would have been even larger.

O−H bond strengths and the character of the corresponding manganese complexes were investigated further in two other recent B3LYP studies.[50,51] In these, the formation of $Mn^{IV}=O$ was also considered. The O−H bond strength in an $Mn^{III}-OH$ complex going to an $Mn^{IV}=O$ complex was computed to be 103.6 kcal/mol. This means that it does not appear to be easier to form a terminal $Mn^{IV}=O$ bond than to form a terminal $Mn^{V}=O$ bond. This point was not fully realized in the previous study on the water oxidation mechanism,[1] as will be discussed further below. Another very important point for water oxidation was also found in these and previous unpublished studies, and this is that a 6-coordinated formally $Mn^{V}=O$ complex actually becomes a $Mn^{IV}-O^{\bullet}$ complex. This is not an arbitrary assignment, but the spin population on oxygen is actually as large as 0.9 and sometimes even larger in these complexes. Perhaps even more remarkably, for a neutral 6-coordinated complex with only hydroxyl and water ligands (with no oxo ligand), manganese still does not want to be Mn(V). Instead it remains Mn(IV) and spreads out one redox equivalent (with negative spin) on two hydroxyl ligands. In contrast, for a 6-coordinated Mn(IV) complex with water and hydroxo ligands, the spin populations on the oxygens do not exceed 0.10 (usually even less than 0.05). The high spin population of 0.9 on the $Mn^{IV}-O^{\bullet}$ complexes is also independent of whether the spin on oxygen is low spin or high spin coupled to the manganese spin. For 6-coordinated $Mn^{IV}=O$ complexes, the spin on oxygen is typically only 0.4. Of equal importance for water oxidation is the fact that the O−H bond strength going from a 6-coordinated $Mn^{IV}-OH$ to an $Mn^{IV}-O^{\bullet}$ complex is quite high, 103.9 kcal/mol, for a neutral complex with hydroxo and water ligands.[51] The splitting between the high-spin and low-spin states is in this case 2.1 kcal/mol. The bond strength is thus higher than the one in tyrosine by as much as 17.4 kcal/mol.

Since the high-spin population was considered to be part of the energetic problem to form these terminal oxo groups, investigations using other ligands were also made. For example, imidazolate ligands were placed cis or trans to the oxo ligand to see if this could relieve some of the spin from the oxo group and thereby make the O−H bond weaker. When the imidazolate was placed trans to the oxo for a 6-coordinated formally $Mn^{V}=O$ complex, the spin on the oxo was indeed reduced from 0.9 to 0.4, but the O−H bond strength actually increased to 105.2 from 103.9 kcal/mol. In this case the imidazolate became a radical with spin 1.0. With imidazolate in the cis-position, the effects on the oxo spin and the O−H bond strength were quite small. One interesting aspect of these imidazolate complexes is that the spin on manganese is reduced by up to 0.3, which could be of importance when the degree of oxidation of the manganese centers is discussed; see further below. Finally, also neutral imidazole ligands were placed cis and trans to the oxo group instead of water. In the case of the cis position for a formal $Mn^{IV}=O$ complex, the effect on the O−H bond strength is a reduction by 2.5 kcal/mol to 101.1 kcal/mol and the oxo spin population is reduced by 0.03. With imidazole trans to oxo instead of water, the O−H bond strength was reduced by 6.8 kcal/mol to 96.8 kcal/mol for the $Mn^{IV}=O$ case and was increased by 3.0 kcal/mol to 106.9 kcal/mol for the $Mn^{V}=O$ case. The spin population on the oxo group was reduced by 0.05 for $Mn^{IV}=O$ and increased by 0.12 for $Mn^{V}=O$. Even if these effects on the bond strengths are not negligible, they are far from sufficient to make the bond weaker than the one in tyrosine of 86.5 kcal/mol.

A very large number of manganese dimer models were also investigated in the two previous studies on the water oxidation mechanism, including several hundred structure optimizations.[1,56] The pattern as described above remains the same. In summary, all previous investigations have led to the result that it is energetically very difficult to form terminal Mn=O oxo bonds, independent of whether $Mn^{IV}=O$ or $Mn^{V}=O$ are formed. This result is also to a certain extent independent on the ligands and on their positioning. Water, hydroxide, imidazole, carboxylate, and chloride ligands were tried in both Mn(IV) and Mn(V) complexes without any success in bringing down the terminal MnO−H bond strength to the one in tyrosine.

b. Previous Oxygen Radical Mechanism for Water Oxidation. Apart from the studies mentioned in the previous subsection, where MnO−H bond strengths in different model complexes were investigated, the problem of formation of the O−O bond has also been studied by B3LYP. In the initial study,[56] already prepared terminal $Mn^{V}=O$ oxo bonds were approached to each other in order to make an O−O bond. In the same study a terminal $Mn^{V}=O$ oxo bond was also moved towards a terminal Mn−O hydroxo bond to form an Mn−OOH ligand. In other unpublished work, attempts to form an O_2 molecule from two bridging μ-oxo oxygens were also tried. Models with 5- and 6-coordinated manganese centers were investigated. For all these model reactions, very high barriers (above 25 kcal/mol) were obtained, in contrast to the barrier of about 10 kcal/mol found experimentally for PSII. There is one reason in common for the high barriers in all cases tried, and this is the difficulty to reach a point where an oxyl group (oxygen radical) is formed. It was always found that very early in the reactions the Mn=O oxo bond was promoted to an $Mn-O^{\bullet}$ oxyl group which for the model complexes tried cost too much energy. Later studies on O−O bond formation were therefore focused on the problem of creating oxyl radicals at a sufficiently low energy cost; see also previous subsection.

After extensive B3LYP investigations an oxyl radical mechanism for O−O bond formation in PSII was formulated.[1] The suggested mechanism includes several new ideas, which were proposed and tested. First, general spin-state considerations were shown to lead to the conclusion that formation of O_2 most probably will require preformation of an oxyl radical, in line with the experience obtained in the initial search for possible transition states described above. The reasoning was as follows. In a typical weak ligand field redox reaction, in which at least one metal atom changes oxidation state, this will lead to a change of ground state spin. The positions of the excited states before and after the reaction are therefore critical. For a low barrier reaction, either the excited state of the reactant corresponding to the product ground state (the high-spin state) or the excited state of the product corresponding to the reactant ground state (the low-spin state) has to be low lying. In the case of water oxidation the reactant excited state (before O−O bond formation) is expected to be an oxyl radical since the ground state has a rather weak second bond to the oxo ligand. This oxyl radical should be very reactive and ideal for formation of the O−O bond. The product excited state, on the other hand, is just a recoupling of the d shell, which should not help O−O

bond formation. This leads to the conclusion that it is the excited state for the reactant that has to be low lying. All model calculations also point in the same direction. In fact, for a sufficiently low barrier, the oxygen radical state of the reactant has to be prepared prior to the step where the O−O bond is formed, which is after the S_3 step. No oxidation of manganese should therefore occur going from S_2 to S_3. In subsequent studies it has furthermore been shown that the oxyl radical appears also on the low spin state of the reactant, which means that the creation of the oxyl radical can not be avoided, either way the reaction occurs.

Another conclusion drawn in the previous study was also that if a terminal oxyl radical should be formed in S_3, then most likely only one manganese center should be redox-active in the water-oxidizing cluster, at least in the critical S_1-S_3 states. The formation of the oxyl radical was found to be considerably complicated by the fact that it cannot be generated by removing a proton and an electron (or hydrogen atom) from an Mn^{IV}−OH group. Breaking the MnO−H bond to form an oxyl radical was found to be much too costly (by about 20 kcal/mol) and is not possible using the driving force from the formation of the TyrO−H bond. This is not unexpected since an oxyl radical is very reactive and will therefore also bind hydrogen atoms very strongly. There is thus the dilemma that Mn−oxo groups can in principle be formed by hydrogen abstraction (see previous subsection for 5-coordinated Mn^{V}═O) but these oxo groups will be unreactive, while the desired reactive oxyl groups cannot be formed by removing a proton and an electron (or hydrogen atom). A possible solution to this problem was suggested to involve the Ca cofactor, which should provide sufficient free energy from chelation to the Mn cluster to allow the formation of the oxyl radical in an indirect pathway. In this pathway a proton is instead abstracted from a water ligand, bridging the Mn cluster and calcium.

Once the oxyl radical has been formed following the indirect pathway described above, there is still the problem of finding a transition state for O−O bond formation. After a considerable number of attempts, a transition state was finally found with a barrier height of only 9.9 kcal/mol in line with the experimental estimate. The suggested O−O bond formation involves an external water apart from the oxyl radical. This mechanism is therefore consistent with recent $H_2{}^{18}O$ labeling experiments showing that of the oxygens forming O_2 one is very rapidly exchanging with solvent water.[18] Finally, in the previous study, the mechanism for formation of the oxyl radical was combined with the mechanism for formation of O_2 to suggest an entire sequence of S states. Although the suggested oxygen radical mechanism solves many of the more significant problems in water oxidation, there are still some questions that need more investigations. Some of these are listed below:

(1) The previous model has only one redox-active manganese atom, and in the calculations actually only one manganese center was used (including also the Ca and Cl cofactors). Since it does not make chemical sense that the other three Mn centers in the water-oxidizing complex should be without a purpose, their function still remains to be found.

(2) The suggested mechanism requires the formation of a terminal Mn^{IV}═O oxo group at S_2 using the driving force of the TyrO−H bond strength. Although this was believed to be possible at the time of the previous study, continued model studies (see previous subsection) have shown that this is far from a trivial point.

(3) The previous model has a terminal Mn^{IV}═O ligand at the same center as there is a water ligand, and it is required that a proton is not transferred between these ligands. It is not clear how that is prevented.

(4) The previous model calculations only considered the steps from S_2 to S_4. For a full understanding of water oxidation, detailed molecular models are required for the full catalytic cycle from S_0 through S_4.

(5) The previous model gives a nice rationalization for why one oxygen of O_2 rapidly exchanges with solvent water. However, the second oxygen in the previous model should be a terminal Mn^{IV}═O in S_2 and an Mn−O(radical in S_3, and it is not clear how this oxygen could exchange even slowly with solvent water which is found experimentally.

c. Mn_3 Cluster Models. A major goal with the present study is to extend the small cluster from the previous study by including more than one manganese center. It should be emphasized from the beginning that the goal is not to construct the actual PSII cluster prior to an experimental X-ray structure, which is an impossible task at this stage, but to build a general model for which general effects can be defined. Some of these effects are then considered likely to be of importance for the actual Mn_4 cluster. When the new cluster was constructed, the 13 points listed in the Introduction were taken into consideration. A larger cluster was built around the single Mn-center complex from the previous study without destroying the major effects found. The new manganese centers introduced will thus mainly lead to new trans-effects, which are investigated one by one. The major trans-effects found are described in the next subsection. Including just the first-order trans-effects leads to a cluster consisting of three manganese centers, and most results discussed in this paper will concern this type of cluster. The position of the fourth manganese center will only briefly be discussed. A main point considered when the new cluster was constructed is that both short Mn−Mn distances increase in the S_2 to S_3 transition (point 3 in the Introduction). A conclusion drawn already at the onset of the present study is that to fulfill this requirement the two Mn dimers have to be neighboring, since a long distance interaction of this type is considered very unlikely. The central manganese atom in the Mn_3 cluster will therefore have four μ-oxo bonds. It is unlikely that all these μ-oxo bonds should be trans to each other, but one trans-interaction is unavoidable. The Mn_3 clusters of present interest will therefore not have a linear arrangement of the three manganese centers, but these centers will form a triangle. A second important experimental result is that there should be two Mn−Ca distances of about 3.5 Å (point 5 in the Introduction). Considering one of these Mn centers to be the central one in the Mn_3 cluster fixes the general structure of the model cluster. With 6-coordinated Ca and Mn centers this leads to the formation of a central cube of the cluster with one missing corner. Two types of Mn_3 clusters fulfilling these general requirements are shown in Figure 2 and will in the rest of the paper be termed models A and B. In the figure a tentative position of the fourth manganese center is also given, but this is clearly quite uncertain.The ligands in the Mn_3 model are initially chosen to be either water or hydroxo ligands apart from the known μ-oxo ligands. This choice is made for simplicity and is based on the fact that most ligands should be oxygen derived. It has previously been found that hydroxyl groups are excellent models for unprotonated carboxylates and water for protonated carboxylates, such as those found in Asp or Glu residues. There are experimental indications for a possible presence also of one or two His ligands in the cluster, but the previous model studies have not indicated any particular electronic properties of these ligands different from those of

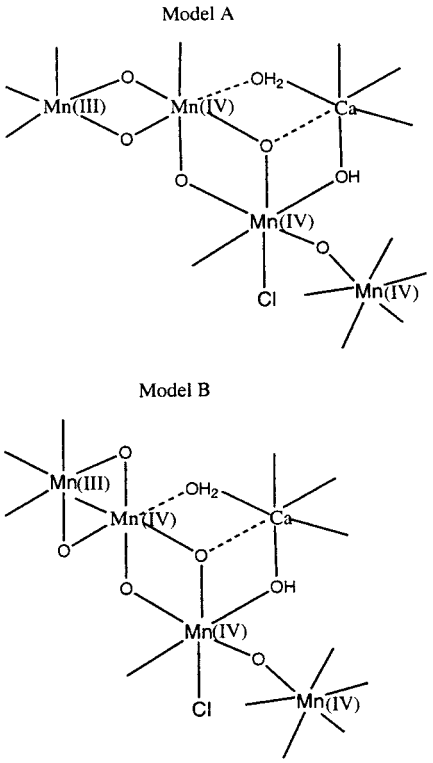

Figure 2. The two forms of the water-oxidizing cluster discussed in the text.

hydroxyl and water groups (see previous subsection). Explicit His ligands were therefore not considered in the present study. A common property of metal complexes embedded in a low-dielectric medium is that they are overall neutral. In the present case it is conceivable that the cluster could have one charge, positive or negative, but this should complicate the initial electron-transfer process from Tyr_Z to P_{680} considerably. The present models will therefore in most cases be chosen neutral. The few cases where charged clusters are used will be explicitly mentioned in the text below. Apart from the general structure of the Mn_3 cluster described above, the explicit choice of hydroxyl or water ligands at each position are tested case by case. The criterion used is that the energy for removing a proton and an electron should be about 86.5 kcal/mol in each S-state transition, in particular for the critical S_2 to S_3 transition. The same requirement is used to decide upon the oxidation states of the manganese atoms of the cluster.

d. Important Trans-Effects for Oxygen Radical Formation. As described above in subsection a, coordination to manganese reduces the O−H bond strengths substantially but not sufficiently in most cases. For the models shown in Figure 2, a few important trans-effects have been noted, which are likely to be of importance also for the actual manganese cluster. These effects, which are some of the main results of the present study, will be described in this subsection in detail. To follow this description, the numberings of the atoms in the Mn_3 model are given in Figure 3 for the optimal structure found for the S_2 state of type model A.

Before the trans-effects are discussed in detail, one of the most important results of the present study should be mentioned. Independent of cluster model investigated, and also independent of the protonation state of the different ligands, the oxygen radical created in S_3 is always found at the O5 position in Figure 3. This is a bridging position in agreement with previous suggestions from EXAFS.[3] This type of position for the radical

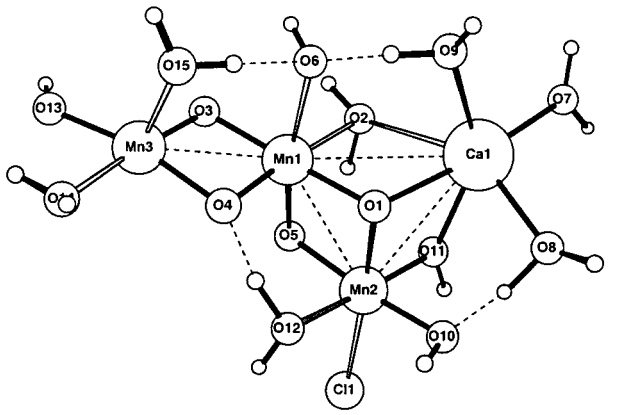

Figure 3. Numbering of the atoms for model A.

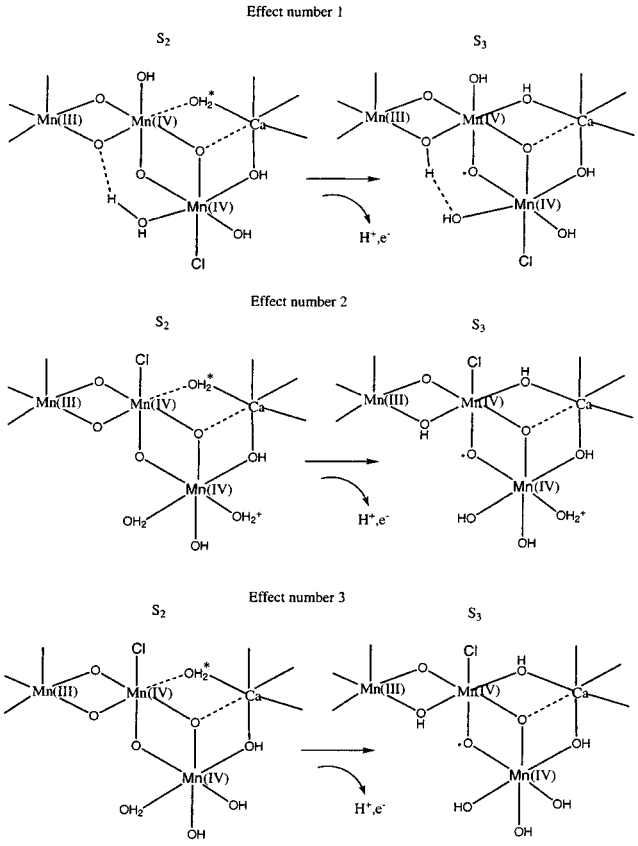

Figure 4. Effects nos. 1−3.

was not investigated in the previous study since only one manganese center was used in the model cluster. A problem pointed out with the previous model is that in S_2 a water ligand is needed at the same time as a terminal oxo ligand (see point 3 in section IIIb), which requires that an energy-gaining proton transfer from the water to the oxo is prevented in some way. This problem is much less severe when the oxo in S_2 is bridging. Manganese complexes with unprotonated μ-oxo bridges are common systems in inorganic chemistry. Another important point, not emphasized in the previous study, is that the spin on the oxygen radical is antiferromagnetically coupled to the manganese spin. Again this type of coupling is difficult to converge (see section II) but was converged for a few cases. The energy gain, compared to the ferromagnetic coupling, is 3.6 kcal/mol. This energy is therefore subtracted from the energy required to reach the S_3 state in all cases discussed below.

The first trans-effect is the most significant one and suggests an explanation for an important experimental observation. This

trans-effect appears in the S_2 to S_3 transition and has direct structural implications. The effect can be explained as follows. In the S_2 to S_3 transition the removal of an electron and a proton should result in the oxyl radical formation. This is the most critical step in the entire water oxidation process, and almost all models tried lead to a too large energy requirement for this step. The only ones so far found fulfilling the energy requirement of 86.5 kcal/mol contain the main features shown as effect number one in Figure 4. In this process, a proton is removed from a water molecule (O2 in Figure 3) bridging manganese and calcium, just as in the smaller models used in the previous study. In both models A and B in Figure 2, the bridging water molecule is trans to a μ-oxo bond between two manganese. When a proton is removed from the bridging water, a hydroxyl ligand results, which has a much stronger trans-effect than the initial water ligand. This increase of the trans-effect would make the transition energetically impossible unless the μ-oxo group can be simultaneously protonated, thus releasing some of the strong trans-effect on the hydroxyl group. This protonation can possibly be achieved if a water ligand (O12 in Figure 3) is placed on the third manganese center hydrogen bonding to the μ-oxo bond as in Figure 4. In the calculations performed on this model, a proton indeed moves automatically from the water to the μ-oxo bond, making the transition energetically possible. Simultaneously, an oxyl radical is created on another μ-oxo group (O5 in Figure 3) bridging two other manganese, as shown in Figure 4. A very important consequence of this effect is that both the short Mn−Mn distances (Mn1−Mn2 and Mn1−Mn3) will increase in the S_2 to S_3 transition, in line with the EXAFS result. It is not easy to find another model rationalizing this surprising experimental result.

The second trans-effect mentioned here is also shown in Figure 4 for the S_2 to S_3 transition. The effect concerns the protonation of the hydroxyl ligand (O10 in Figure 3) of the bottom Mn(IV), trans to the oxyl (O5) formed in S_3. The trans-effect of the hydroxyl group should be much smaller for the oxyl in S_3, which binds weaker to Mn(IV) than the oxo group does in S_2. A protonation of this hydroxyl group is therefore expected to increase the energy required to remove an electron and deprotonate the bridging water. The calculations confirm this expectation and show that the effect is actually as large as 8.0 kcal/mol. In other words, the O−H bond strength of the bridging water (O2) is 8.0 kcal/mol stronger when the hydroxyl group O10, which is at the other end of the cluster, is protonated. This is a quite remarkable result and shows the sensitivity of the critical O−H bond strengths to structural features of the cluster even quite far away from the O−H bond.

The third trans-effect again concerns the ligands trans to the oxyl (O5) formed in S_3 and is shown in Figure 4. Compared to the structures shown as effect number 1 in the figure, which represent the optimal structures, the structures showing the third effect are formed by switching the hydroxyl ligand (O6) on the central Mn(IV) trans to the oxyl, with the chloride ligand at the bottom Mn(IV) trans to the second μ-oxo bond. Since chloride is a weaker trans-ligand than hydroxyl, this switch is expected to increase the energy required for the S_2 to S_3 transition. The calculations show that the increase is 8.2 kcal/mol, which is surprisingly large. This effect is, in fact, the only effect seen in any of the present model calculations showing that the position of the chloride ligand is important. All other investigations replacing chloride with similar ligands have given very small effects; see further section IIIf.

The fourth effect concerns the importance of the leftmost Mn(III) center (Mn3) and is shown at the top in Figure 5. In this

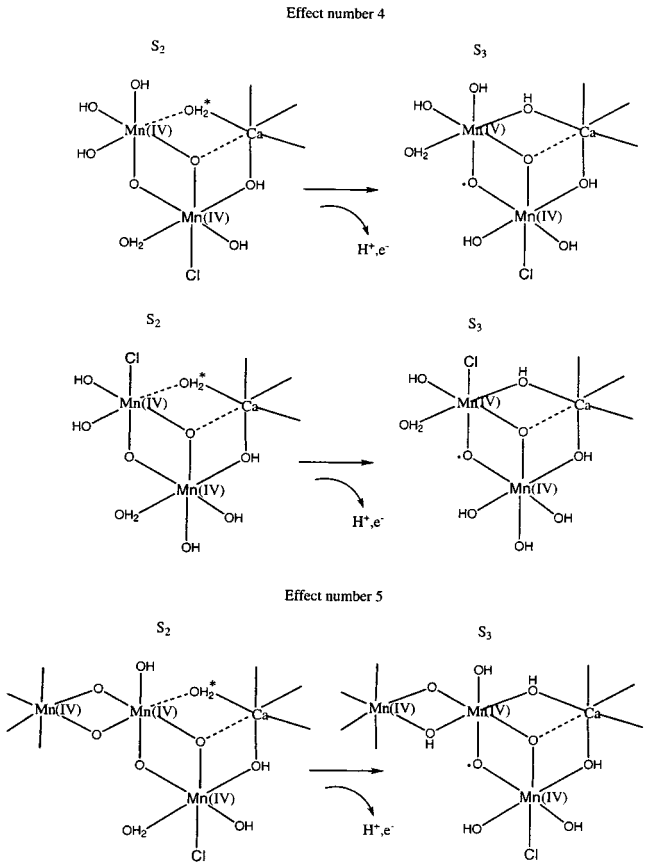

Figure 5. Effects nos. 4 and 5.

model calculation the Mn(III) center was simply removed and the two μ-oxo bonds (O3 and O4) were replaced by hydroxyl groups to keep the overall neutral charge of the cluster and the oxidation states for the other two manganese centers. The calculated effect of removing the Mn(III) center is an increase by 10.5 kcal/mol for the S_2 to S_3 transition. There are many contributing effects for this total energy increase. Apart from the obvious change of ligand trans to the bridging water (O2), a major part of the energy increase is due to the hydroxyl ligand (O6) trans to the oxyl on the upper Mn(IV), as judged by the distance changes. The trans-effect for this ligand is essentially unchanged in S_2 but is much stronger in S_3 when Mn(III) is removed. The reason for this is that the hydrogen bond to this ligand from the water (O15) on Mn(III) is missing. This is partly compensated in S_2 by a much stronger hydrogen bond to the water (O9) on calcium but is not compensated in S_3. This fourth ligand effect is one of the best examples found in the model calculations showing that a manganese center can be very important for water oxidation even though its oxidation state is never changed.

For the Mn_2 -cluster model, where the Mn(III) center was removed, an additional set of calculations was performed. As for trans-effect number 3, the hydroxyl group (O6) was switched with the chloride ligand, as shown at the bottom of the fourth effect in Figure 5. This led to an additional increase of the energy required for the S_2 to S_3 transition by 7.7 kcal/mol, compared to an effect of 8.2 kcal/mol for the Mn_3 cluster model. The most interesting aspect of this calculation is that the two effects found for the Mn_2 cluster are additive, leading to a total energy effect of 18.2 kcal/mol, when the Mn(III) center is removed and the hydroxyl and chloride ligands switched. This is a quite remarkable result and moves the O−H bond strength of the bridging water (O2) a long way from the one in tyrosine of 86.5 kcal/

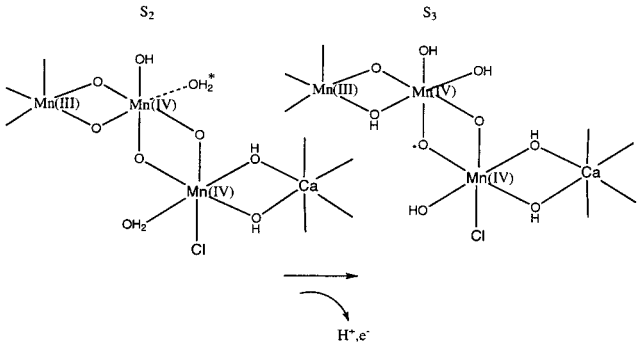

Figure 6. Effect no. 6.

mol toward the one of free water of 118 kcal/mol. Clearly, to achieve a sufficiently small O−H bond strength, a number of significant structural elements of the manganese cluster have to be tuned. This represents, in fact, the basis for making the present type of investigation meaningful. With very many small effects of only 1−3 kcal/mol, calculations on hypothetical clusters would hardly be worthwhile.

The tests performed for trans-effects number 4 showed that the presence of the third manganese center (Mn3) is quite essential. A question is then if also the oxidation state of this center is important. To test this, the oxidation state was changed from Mn(III) to Mn(IV). Since Mn(IV) prefers 6-coordination, an additional ligand was also placed on this center, shown as effect number 5 in Figure 5. The result of this test is that the energy requirement for the S_2 to S_3 transition increases by 6.6 kcal/mol. Apparently, the nature of the μ-oxo bonds (O3 and O4) changes character sufficiently to cause this quite significant effect. There is also some change of the hydrogen-bonding capability of the O15 water as the Mn3 center changes from Mn(III) to Mn(IV). This water ligand is relatively free for Mn(III), being along the weak Jahn−Teller axis, and therefore does not change character during the S_2 to S_3 transition, while for Mn(IV) there is a substantial change of character during this transition. Apart from this change, the changes of the bond distances are all quite small, indicating that the energetic effect is spread out on many different bonds. Effects numbers 4 and 5 clearly show that the character of the Mn3 center rather strongly affects the energy for the S_2 to S_3 transition. A question is then if also the fourth manganese center, omitted in the present models but indicated in Figure 2, could have effects of a similar size. Since this manganese center is suggested to be only loosely connected to Mn2 (not Mn1) by a single μ-oxo bond, this appears very unlikely. In contrast, Mn3 is strongly connected to Mn1 through two μ-oxo bonds which should have, and are shown to have, major trans-effects on the water from which the proton is being removed going from S_2 to S_3. However, small effects from the fourth manganese center cannot be ruled out.

The final effect mentioned here, representing trans-effect number 6, concerns the chelating effect of calcium and was tested for the S_2 to S_3 transition as shown in Figure 6. In the original structure of the first effect in Figure 6 there is a direct bonding between calcium and the bridging water O2. Moving calcium away from this water down toward the Mn2 center, binding to this center through the O10 and O11 hydroxyl groups, leads to an energy increase for this transition by 8.0 kcal/mol. This result is not surprising since the calcium should bind better to a bridging hydroxyl in S_3 than to a bridging water in S_2 in the original position in the first effect of Figure 4, while this additional chelating energy is not used in the structure in Figure 6. This type of chelating effect was already pointed out as

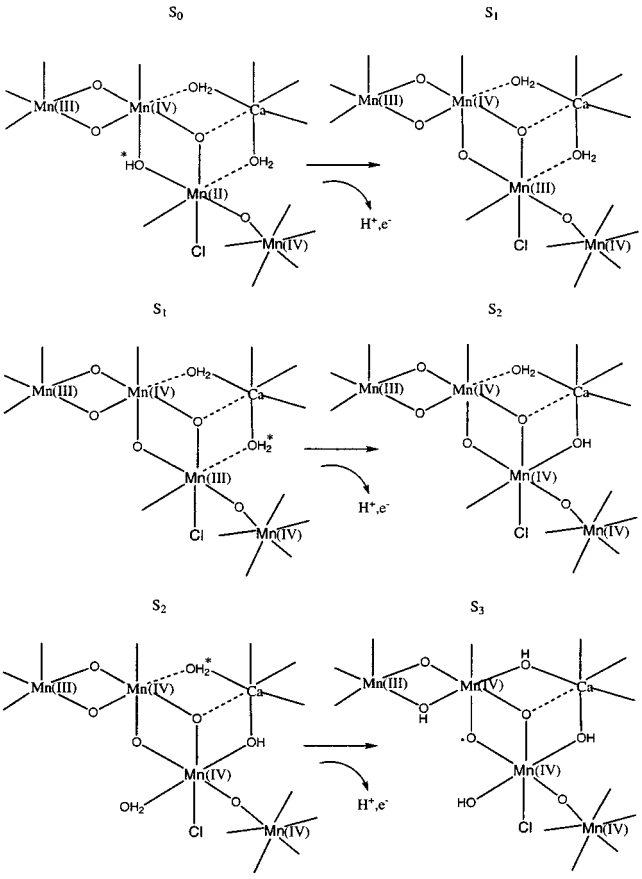

Figure 7. Suggested schemes for the different S-state transitions. H* marks the proton that is being removed in each transition.

essential in the previous smaller model study and still represents one of the basic ideas for the role of calcium in water oxidation in the oxyl radical mechanism for larger cluster models.

It should finally be added that the above effects are only a fraction of the effects investigated for the Mn_3 model cluster. Most of the effects were also tested for the model B type, shown in Figure 2, with very similar results. In fact, at the present stage no significant difference is found between models A and B, and it is therefore yet impossible to conclude which of these should more closely correspond to the actual cluster.

e. Suggested S-State Transitions. The consideration of the trans-effects discussed in the previous subsection led to optimal Mn_3 structures for S_2 and S_3 as shown in Figure 4 (illustrating trans-effect number 1). In a somewhat less complete investigation of optimal ligand positions and trans-effects for the lower S-states, suggestions could also be made for the S_0 to S_1 and S_1 to S_2 transitions. All the lower S-state transitions will be described in this subsection in sequential order including the energetic requirements and structural changes.

The suggested S_0 to S_1 transition is shown in Figure 7. The first point that should be noted about this transition is that the redox-active center is not the central one (Mn1 in Figure 3) but the bottom one (Mn2). This result came out quite clearly from the model investigations. If an Mn(II) center is placed in the center of the cluster, this led to two rather long Mn−Mn distances in S_0. As this center is oxidized from Mn(II) to Mn(III) in the S_0 to S_1 transition, this in turn led to a decrease of both these distances. This result is not in agreement with EXAFS measurements showing that only one of the Mn−Mn distances decreases (see point number 4 in the Introduction), and a central position for Mn(II) in S_0 can therefore be ruled out.

Having defined the position of the redox-active center in the S_0 to S_1 transition, there still remains to suggest the proton being removed. The EXAFS measurements suggest that one of the μ-oxo bridges should be protonated in S_0 but not in S_1, and this position is also the best suggestion for the removal of a proton from the present investigation. Protonation of the O5 oxygen in the lower left corner in the incomplete cube leads to an energy requirement for this transition of 77.6 kcal/mol, well below the TyrO−H bond strength of 86.5 kcal/mol, as required. The alternative protonation of the O1 μ-oxo bridge cannot be ruled out but would most likely require two proton abstractors in the deprotonation processes; see further below.

The next S-state transition, from S_1 to S_2, is suggested to occur as shown in Figure 7. The proton to be removed is more or less already defined by the detailed investigations of the S_2 to S_3 transition described above, which determine the best structure of the S_2 state. This proton is one at the O11 oxygen at the bottom right corner in the incomplete cube. The S_1 to S_2 transition should then be substantially helped by a similar chelating Ca effect as the one for the S_2 to S_3 transition, discussed as effect number 6 above. The calculated energy requirement for this transition is 79.7 kcal/mol, again well below the TyrO−H bond strength of 86.5 kcal/mol. It should be added that, with such a low transition energy, it may not be absolutely essential to use the chelating Ca effect, which may open up other possibilities for the cluster structure. Calcium might then instead be positioned between the central Mn and the loosely connected Mn(IV) center that is tentatively indicated in the figures. This position would remove the Ca-chelating effect for the S_1 to S_2 transition, but it would still be present in the critical S_2 to S_3 transition.

The S_2 to S_3 transition has already been discussed in detail above, but is shown again in Figure 7. The calculated energy for this transition is 86.9 kcal/mol, sufficiently close to 86.5 kcal/mol to be viable. This transition is thus suggested to be the most difficult one, in line with experimental suggestions, and would have almost no driving force. All positive trans-effects discussed in the previous subsection are needed to make this transition low enough. The oxyl radical appears in the μ-oxo position O5 in S_3. In summary of the three lowest S-state transitions, protons are suggested to be abstracted from three corners of the incomplete cube. With this suggestion, a single proton abstractor such as a tyrosyl radical or a base situated at the empty corner of the incomplete cube is a possibility.

The optimized geometries for the different S states are given in Figures 8 and Figure 9. Going from the S_0 structure to the S_1 structure in Figure 8, one of the Mn−Mn distances does not change much, from 2.77 to 2.74 Å, while the second one changes much more, from 3.07 to 2.82 Å, in line with EXAFS interpretations. The two Mn−Ca distances are 3.5 and 3.6 Å in S_1 in line with strontium EXAFS giving two distances of about 3.5 Å in S_1. One of these distances is calculated to be slightly longer in S_0, with 3.8 Å. It should be added that, with the present basis sets, the Mn−Ca and Mn−Mn distances are expected to be slightly long.

For the S_1 to S_2 transition, both Mn−Mn distances remain rather constant. One of them is 2.74 Å in both S states, while the other one changes slightly from 2.82 to 2.80 Å. In the S_2 to S_3 transition both Mn−Mn distances increase in line with EXAFS interpretations. One of them increases by 0.07 Å from 2.74 to 2.81 Å due to protonation of a μ-oxo bridge, while the other one increases by 0.13 Å, from 2.80 to 2.93 Å due to the presence of the bridging oxyl radical in S_3.

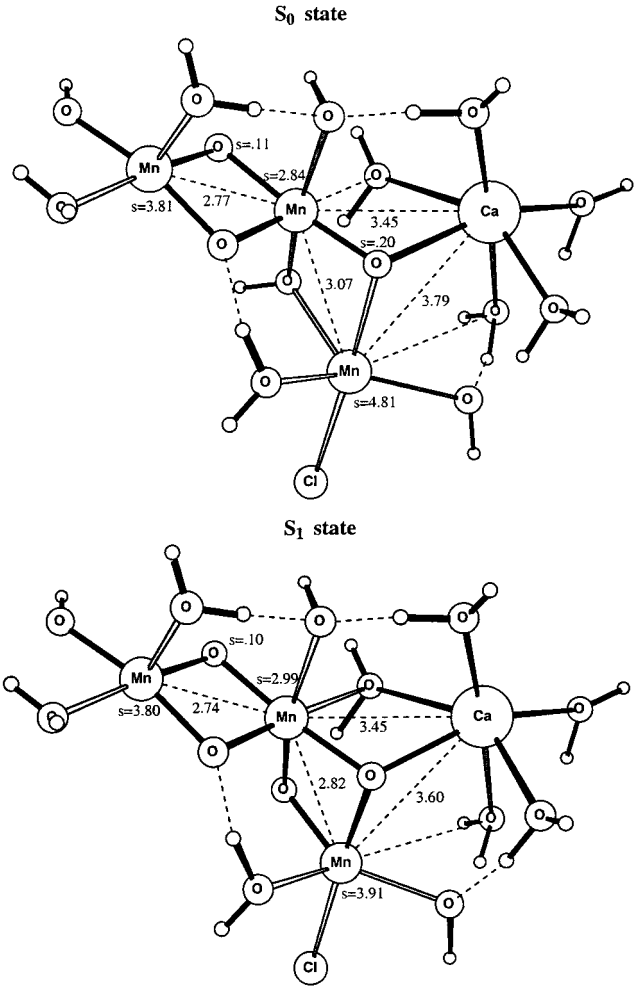

Figure 8. Optimized structures for the S_0 and S_1 states of model A. Spin populations larger than 0.10 are marked.

The Ca-chelating effect is clearly seen on the Mn−Ca distance changes both in the S_1 to S_2 and S_2 to S_3 transitions. In the first of these transitions one Mn−Ca distance decreases by 0.35 Å, from 3.60 to 3.25 Å, while the other one remains essentially constant. Since a change of 0.35 Å is quite large and requires a large motion of the bridging hydroxyl, a calculation was also performed for a negative complex for S_1 (one of a very few charged models in the present study), but the distance change remained equally large. In the S_2 to S_3 transition the other Mn−Ca distance changes by 0.21 Å, from 3.51 to 3.28 Å, while the first one remains almost constant. As discussed above, these compressions of the cluster are due to the better bridging ability of hydroxyl than of water ligands.

There is a slight remaining problem in the comparison with the EXAFS measurements, and this concerns the relative length of the short Mn−Mn distances in the S_1 and S_2 states. In S_1 the optimized distances differ by 0.08 Å, while in the S_2 state the difference is 0.06 Å. Experimentally these distances should be more equal. The reason for the discrepancy is the strong Ca−O1 connection which makes the Mn1−Mn2 distance slightly longer than the other one. Several attempts have been made to find structures where the Ca−O1 contact is weaker or absent. One attempt was to make calcium 7-coordinated by placing another water in the region of O1. Doing this led to only a very small change of 0.2 kcal/mol for the energetic requirement for the S_1 to S_2 transition, so this is energetically possible. The

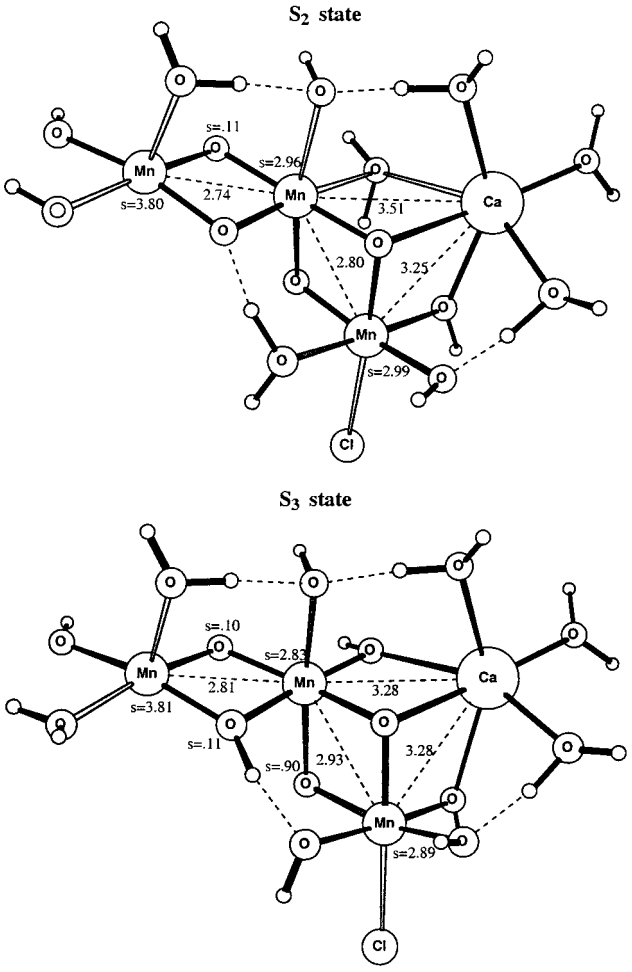

Figure 9. Optimized structures for the S_2 and S_3 states of model A. Spin populations larger than 0.10 are marked.

additional water did not lead to a disappearance of the Ca−O1 contact but to a significant weakening of the Ca−O2 contact instead. It also had the effect that the short Mn−Mn distances became slightly more equal, the difference going down from 0.08 to 0.04 Å in S_1 and from 0.06 to 0.04 Å in S_2. Further changes of the Ca−ligand structures, possibly involving other types of ligands, could well lead to additional decreases of the differences in these distances. The possibility to avoid the Ca−O1 contact by placing Ca higher up between Mn1 and the fourth manganese (positioning this manganese above Mn1) was already mentioned above. This would increase the energy requirement for the S_1 to S_2 transition since the Ca-chelating effect would not be present. However, if the increase in the energy requirement is not too large, this may even be an advantage, since the transition energy using the present structures is quite low. An alternative positioning of calcium could also lead to a different angle between the two Mn−Ca interactions, where EXAFS at present suggests that these directions are close to parallel, while the present structures give an angle of about 50°. However, this information from EXAFS must at present be regarded as quite uncertain. Investigations of other types of structures are in progress, but have so far led to too high energy requirements.

The work to find the best pathway for O_2 formation starting from the present S_3 structure is still in progress. Only a few preliminary results with relation to experiments will be given here. First, the position of an external water was investigated and an optimal place at the missing corner of the incomplete

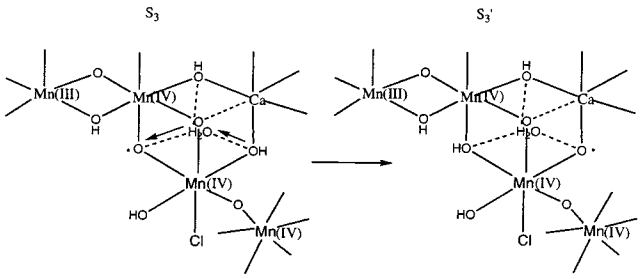

Figure 10. Suggested scheme for the transfer of a radical in S_3.

cube was found. The calculated binding energy for this water is rather high, 10.6 kcal/mol, in fortuitously good agreement with the experimental estimate of 12 kcal/mol based on solvent exchange using labeled oxygens.[57] In the same experiment the second oxygen making up O_2 should be much stronger bound. If this oxygen should be the oxyl radical at the O5 position, the question remains how this oxygen could exchange with water at all. This problem turns out not to be too difficult. The calculations show that the external water in the missing corner of the cube can help transferring the radical character from O5 to both O2 and O11, by a concerted deprotonation of one of these sites and a protonation of O5, with only a small barrier, as shown in Figure 10. Since oxygen (^{18}O) exchange with solvent should not be difficult between a hydroxyl ligand and water, anyone of O5, O2, or O11 could be the second oxygen of the final O_2. It should finally be added that the positioning of the external water at the missing corner of the cube may appear to be in conflict with an optimal positioning of a proton (or hydrogen atom) abstractor like the tyrosyl radical in the same corner. There are a few possibilities out of this apparent dilemma. One is simply that there is not a single but several proton abstractors positioned outside the corners of the cube. A second possibility is that the abstractor takes the protons (or hydrogen atoms) via the water molecule. It is unlikely that this should severely increase the barrier for the abstraction. A third alternative is that the abstractor moves out as water moves in, in S_3.

In the investigations done at present for the O_2 formation there are still several alternatives. One promising possibility is that the O_2 formation starts by the transfer of the radical as in Figure 10. From this position a proton can be transferred from the external water to O2, and the O−O bond is formed at O11 producing an O_2 H ligand. This reaction appears to be slightly endothermic. In the final step the proton of the O_2H ligand is removed by the proton abstractor, as usual concerted with an electron transfer to Tyr_Z. In this process, the O_2 ligand formed is exchanged with an external water and the catalytic cycle is complete. Since there are several other alternatives which need to be carefully investigated, this suggestion is only very preliminary at this stage.

f. Comparison of Different Models for the S-State Transitions. As mentioned above, two different types of Mn_3 models, model A and model B in Figure 2, fulfill the main requirements set by experiments. The energetic requirements for the S-state transitions have been calculated for both models, and the results are shown in Figure 11. The point denoted S_4 is arbitrarily chosen as the structure where a bridging O_2H ligand has been formed at the O5 position, which is the same position as that of the oxyl radical in S_3. Whether this structure will turn out to be on the optimal reaction path remains to be determined, but

(57) Hillier, W.; Messinger, J.; Wydrzinski, T. *Biochemistry* **1998**, *37*, 16908−16914.

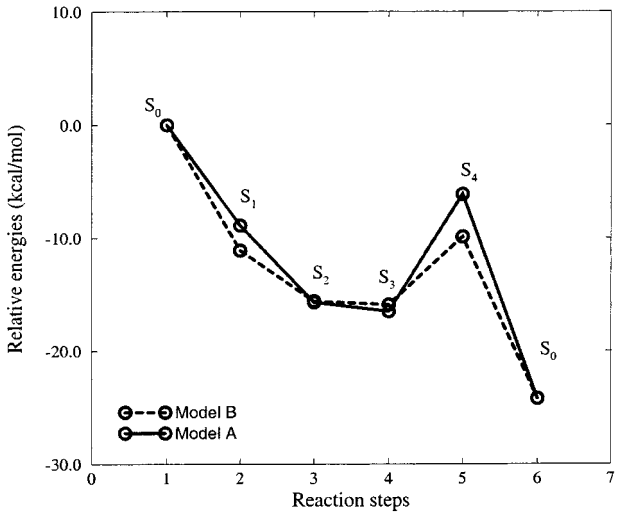

Figure 11. Comparison of the energetics of the S-state transitions for models A and B.

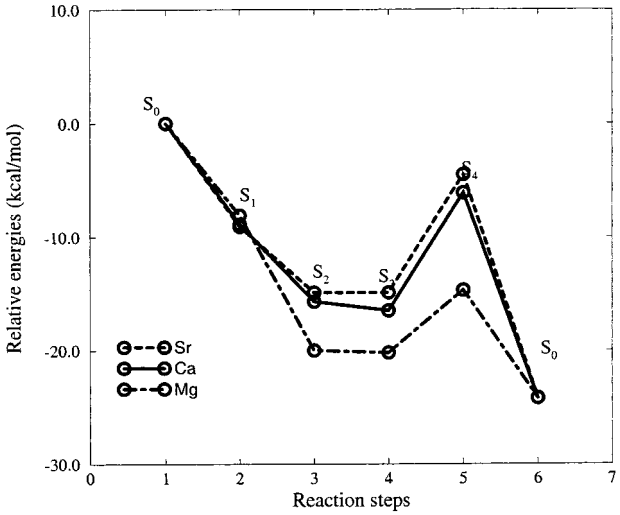

Figure 12. Comparison of the energetics of the S-state transitions for Sr, Ca, and Mg.

the energy should still be representative for comparing different models. As can be seen in Figure 11, the energetic requirements for models A and B are very similar, and it is at this stage therefore not possible to discriminate between these models. The general features of the curves can be described as follows. The first transition between S_0 and S_1 is the most exothermic step in the cycle in line with the general expectations on the basis of experiments. The S_1 to S_2 transition is also exothermic while the S_2 to S_3 is almost thermoneutral. The latter energy is not quite in agreement with experiments which indicate an exothermic transition, but this transition is still the most critical one of the cycle. In going from S_3 to the S_0 of the next cycle, there is a driving force of about 8 kcal/mol and the process has a barrier probably in the range 10−15 kcal/mol. The entire catalytic cycle is estimated to be exothermic by 24 kcal/mol (obtained from experimental heats of formation and the bond strength of 86.5 kcal/mol for the O−H bond strength of tyrosine).

When an estimated energy curve has been obtained for the full water-oxidizing cycle, it is also of some interest to investigate what happens if the Ca cofactor is replaced. In Figure 12, the energy curves obtained for model A when calcium is replaced by strontium and magnesium are compared to the curve for calcium. For simplicity, exactly the same S transitions were compared, using the same type of structures (although reoptimized) and removing the same protons. Experimentally, it is known that only strontium can replace calcium, although with somewhat reduced activity (see point 6 in the Introduction). In line with this finding, the energy curves for strontium and calcium are very similar. The only difference in the structures is that the Mn−Sr distances are about 0.1 Å longer than the Mn−Ca ones. The electronic structure, as for example given by the spin populations, is almost identical for the two cases. The curve for magnesium deviates considerably more from the calcium curve than the strontium curve does. The difference can be easily explained by the distance changes, where the Mn−Mg distances are considerably shorter by about 0.3 Å than the Mn−Ca ones. As expected, this leads to a larger chelating effect for the S_1 to S_2 transition which becomes more exothermic for magnesium. More surprisingly, the energetics for the S_2 to S_3 transition is much less affected. The increased exothermicity for the S_1 to S_2 transition leads to a weaker driving force and thereby probably a higher barrier for the O−O bond formation step in the magnesium case, which might explain why O_2 does not form. (Note that the point denoted S_4 in Figure 12 does not represent a barrier but only a possible point on the reaction pathway.) However, in the case of magnesium more likely explanations for the lack of activity are perhaps that an entirely different complex may be formed or that other protons are more favorable to remove than the ones found optimal for calcium. No investigations of that kind have been performed.

IV. Conclusions

The present study has investigated the oxygen radical mechanism for water oxidation in PSII with larger clusters than previously used. For these larger models, the presence of only one redox-active manganese still appears most probable. The main result of the present study is that, even with a mechanism such as the present one with only one redox-active manganese, the presence and positions of the other manganese centers are quite critical. Properly tuned trans-effects are found to be of large importance for the creation of the oxygen radical. The most striking of these effects is the one that leads to an elongation of both short Mn−Mn distances in the S_2 to S_3 transition in agreement with EXAFS experiments. One of these elongations is caused by a protonation of a μ-oxo bridge between two manganese centers by a ligand on a third manganese center. The second elongation is caused by the creation of the oxygen radical itself. The simplest organization of the manganese cluster allowing for this trans-effect is one where three of the four manganese centers are strongly coupled by μ-oxo bridges in a bent configuration.

A sequence of S states is proposed in which the protons are removed from ligands in the corner of an incomplete cube with a missing corner. This should be regarded as one possibility which is found to fulfill most of the requirements set by experiments and theory. Most of all, the suggested S sequence shows that it is energetically possible to create an oxygen radical in S_3. This is in fact the only one that fulfills this energetic criterion out of a very large number tried so far, of which most were found to be very far away from being feasible mechanisms. This does not mean that this mechanism has to be the one used by nature but is probably as far as it is possible to reach without an experimental structure of the cluster. At least, it shows that an oxygen radical mechanism is possible and it also gives a rationale for the presence of many manganese atoms and a

calcium in the complex even though only one manganese is redox-active, which was the main goal of the present study. With the present limited and partly contradicatory information from experiments, it is unlikely that the present structures are correct in all respects, but as more information becomes available, improved models which can be treated quantum mechanically can be obtained, and some of the conclusions can then be confirmed or modified.

IC9911872